Korean J. Chem. Eng., 33(2), 669-677 (2016)
DOI: 10.1007/s11814-015-0156-1

pISSN: 0256-1115
eISSN: 1975-7220

Polypyrrole-polyaniline/Fe_3O_4 magnetic nanocomposite for the removal of Pb(II) from aqueous solution

Amirhossein Afshar*, Seyed Abolfazl Seyed Sadjadi*,†, Afsaneh Mollahosseini*, and Mohammad Reza Eskandarian*,,***,****

*Faculty of Chemistry, Iran University of Science & Technology, Tehran, Iran
**Department of Applied Chemistry, Faculty of Chemistry, Semnan University, Semnan, Iran
***Department of Chemistry, University of Zanjan, Zanjan, Iran
****Zanjan Zinc Khalessazan Industrial Companies (ZZKICO), Zanjan, Iran
(*Received 1 January 2015 • accepted 20 July 2015*)

Abstract−Lead ion which is engaged in aqueous solution has been successfully removed. A novel technique was utilized for the separation and absorption of Pb(II) ions from aqueous solution. Magnetic Fe_3O_4 coated with newly investigated polypyrrole-polyaniline nanocomposite was used for the removal of extremely noxious Pb(II). Characteristic of the prepared magnetic nanocomposite was done using X-ray diffraction pattern, Field emission scanning electron microscopy (FE-SEM), Fourier transform-infra red spectroscopy (FT-IR) and energy dispersive x-ray spectroscopy (EDX). Up to 100% adsorption was found with 20 mg/L Pb(II) aqueous solution in the range of pH=8-10. Adsorption results illustrated that Pb(II) removal efficiency by the nanocomposite increased with an enhance in pH. Adsorption kinetics was best expressed by the pseudo-second-order rate form. Isotherm data fitted well to the Freundlich isotherm model. Upon using HCl and HNO_3, 75% PPy-PAn/Fe_3O_4 nanocomposite, desorption experiment showed that regenerated adsorbent can be reused successfully for two successive adsorption-desorption cycles without appreciable loss of its original capacity.

Keywords: Polypyrrole-polyaniline, Nanocomposite, Lead, Heavy Metals, Fe_3O_4, Kinetic

INTRODUCTION

Globally, heavy metals such as Cr, Hg, Cd, Ni, Co and Pb are nominated as most influential sources of the environmental contamination. The presence of above-mentioned heavy metals in high concentration in both natural water and wastewater supplies is a threatening menace to health and environmental issue due to their toxicity and bioaccumulation through the food chain and consecutively in the human body. Discussing the removal of heavy metals from environment is absolutely subtle yet intricate. It is subtle because it is obvious to anybody in the world that is urgent to remove the mentioned toxic heavy metals and also is intricate because omitting these contaminants is not so easy. Undoubtedly, among the above-cited heavy metals Pb is a major contaminant because of so many dangerous aspects which dictates to nature and also humans. Pb is extensively used in many industrial procedures such as batteries, gasoline, ceramic industry, military usages, nuclear power plant, dying and other usages [1,2]. In aqueous solution Pb exists in bivalent (Pb(II)) form. Pb(II) is extremely mobile in the environment and so toxic, carcinogenic and mutagenic to living organisms [3,4]. Effluents from certain industries often contain values higher than those and, therefore, it is necessary to reduce the Pb(II) concentration to acceptable level before discharging into the environment. In recent decades a number of technologies have been engaged to reduce/remove Pb(II) from aqueous solutions such as chemical redox followed by precipitation, ion exchange, uses of the different types of membranes, electrodialysis and adsorption [5,6]. The major drawbacks associated with precipitations include large consumption of reagents, high volume of sludge generation and inefficient recovery of treated metals for reuse [7]. Ion exchange, membrane processes and electrodialysis are not economically attractive because of their high operational costs [8]. Of these technologies, adsorption is a versatile and cost-effective technique for the removal of contaminants from water and hence has attracted interest in recent investigations [9-11]. Various adsorption media have been widely used for Pb(II) removal, including activated carbon from different sources [12-14], biomaterials [15,16], metal oxides [17,18], hydrous metal oxides [19-21] and hybrid materials [22], among others. Recently, nanostructured materials have been used for Pb(II) removal from water/wastewater and have proven advantageous over traditional adsorbents due to very large surface area, accessible active sites and a short diffusion length, which result in high adsorption capacity, rapid extraction dynamics and high adsorption efficiencies [23,24]. However, most nanomaterials have some limitations in adsorption and separation of pollutants from large volume of environmental samples. When column dynamic separation mode is used, the nanosized particles packed on a col-

†To whom correspondence should be addressed.
E-mail: seyedsadjadi@iust.ac.ir,
seyedabolfazl.seyedsadjadi@yahoo.com

umn demonstrate high back pressure, and due to this pressure it would be difficult to achieve high flow rates. And in case of stationary batch style, nanosized adsorbents lead to a very low consequent filtration rate [25]. Therefore, it is advantageous to develop a well dispersed nanoadsorbent with large surface area and suitable surface functionality that can remove Pb(II) from large volume of environmental water. The application of magnetic nanoparticles has attracted attention to solve environmental problems [7,26,27]. This is because magnetic nanoparticles besides having large surface area are highly dispersible in water and exhibit super paramagnetic properties. The latter property makes them separable from aqueous solution by the application of external magnetic field [28]. As such, studies have explored application of different nanosized magnetic particles for the removal of Pb(II) from water. The materials studied include maghemite, magnetite (Fe_3O_4), diatomite supported/unsupported magnetite nanoparticles and surface-modified jecobosite nanoparticles [29-31]. Most of these magnetic nanomaterials, however, have low capacities for Pb(II) [5,29,30]. It is therefore imperative to develop new materials with improved capacity for Pb(II). Present study involves using iron oxide (Fe_3O_4) nanoparticles encapsulated by polypyrrole-polyaniline to achieve a well dispersed sorbent that can be magnetically separated and has a high capacity for Pb(II). Previously, polyaniline nanocomposite has attracted much attention due to its unique properties of high electrical conductivity, relatively good environmental immovability, nontoxicity, moderately low cost and ease of preparation, which are favorable for various types of applications [32,33]. However, polyaniline carries charges via some of positively charged nitrogen atoms in the polymer matrix. To maintain charge neutrality, some of the counterions are incorporated into the growing polymer chain [34]. The existence of positively charged nitrogen atoms in polyaniline provides a good prospect for its applications in adsorption or filtration separation [35,36]. Also, polyaniline and polypyrrole have been examined for adsorption purposes, and a more efficient system was needed [37-39]. In present work, for the first time, polypyrrole-polyaniline/Fe_3O_4 nanocomposite has been utilized as an effectual sorbent with enhanced capacity for Pb(II) removal. It is the first usage of the polypyrrole-polyaniline composite beside of Fe_3O_4 nanocomposite due to utilizing in adsorption/desorption procedure for water treatment.

EXPERIMENTAL PROCEDURE

1. Materials

Pyrrole (Py), aniline (An), potassium peroxydisulphate, sodium hydroxide, lead (II) nitrate, hydrochloric acid and ethanol as chemicals were purchased from Merck (Germany). All of the chemicals were in analytical grade and used without further purification. Required

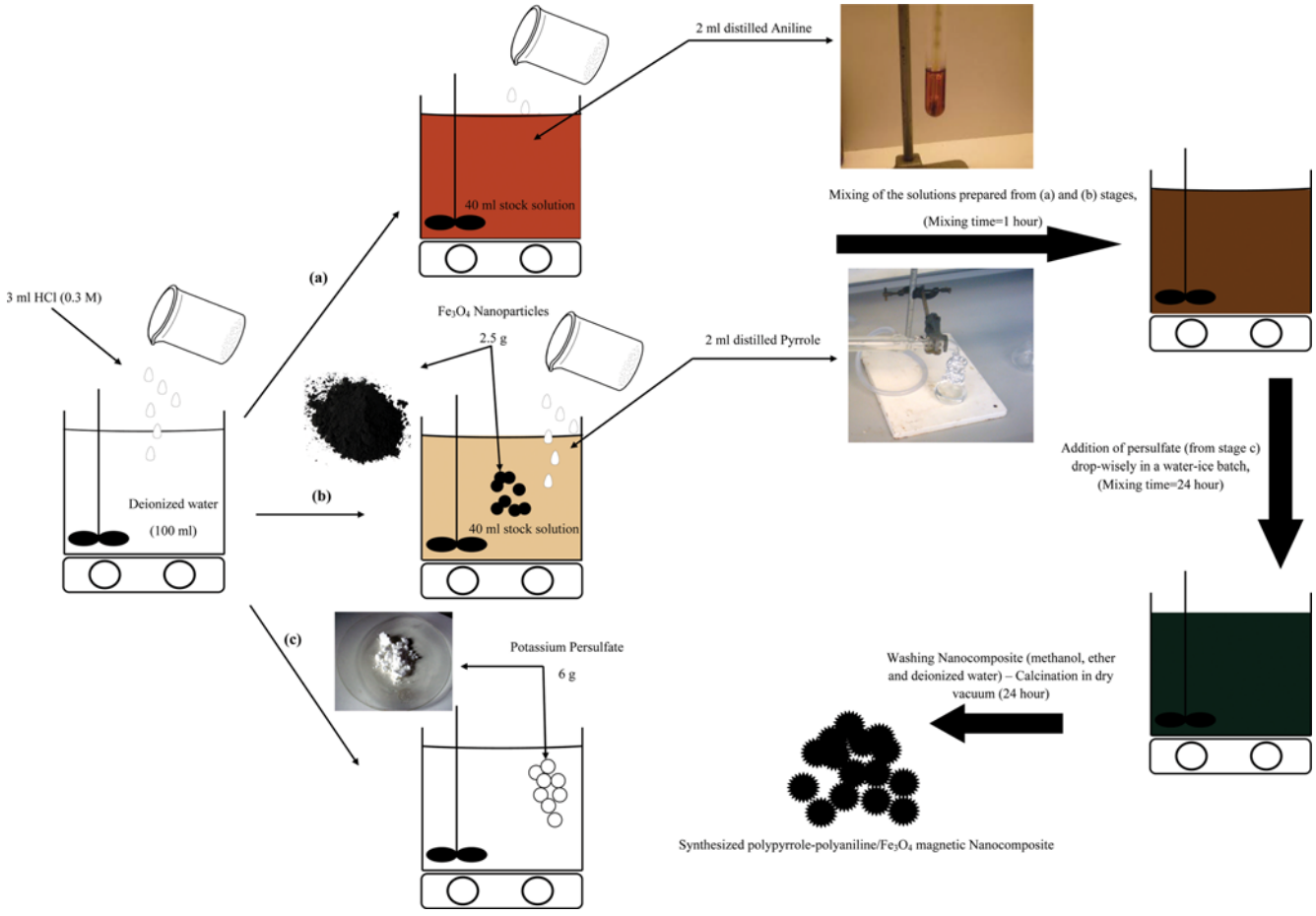

Fig. 1. Schematic representation of the polypyrrole-polyaniline/Fe_3O_4 magnetic nanocomposite synthesis procedure.

Fe_3O_4 nanoparticles for nanocomposite synthesis were purchased from Aria Vajd Company (Tehran, Iran). All other chemicals used in this study were of analytical grade and were freshly distilled before use.

2. Synthesis of the Polypyrrole-polyaniline/Fe_3O_4 Nanocomposite

Nanocomposite was synthesized using previously investigated ideas [38]. Due to synthesis of nanocomposite 3 ml HCl 0.3 M was added to 100 ml of deionized water. So, 2 ml of distilled aniline was added to 40 ml of the above-mentioned solution and also 2 ml of distilled synthesized pyrole and also 2.5 g of nano particles of Fe_3O_4 was added to another 40 ml amount of the first solution (HCl 0.3 M). Two prepared solutions were mixed together and shaken for 1 hour; 6 g of potassium peroxydisulphate was added to the 20 ml of remained amount of first solution and continuously decanted to the mixture of pyrole and aniline solutions in water and ice bath. Mechanical mixing was continued for 24 h and after that the solution was decanted and synthesized polymer which had black to greenish color was washed three times by methanol, ether and deionized water, respectively. Produced nanocomposite was dried at vacuum conditions (40 °C) for 24 h. Synthesized compound was polypyrrole-polyaniline/Fe_3O_4 nanocomposite which had magnetic properties. Schematic representation of the nanocomposite synthesis procedure is illustrated in Fig. 1.

It is noteworthy that polypyrrole also has been successfully copolymerized with other polymers by chemical and electrochemical polymerization [40,41]. Polypyrrole can also be synthesized chemically and electrochemically. It has also been copolymerized extensively with polyaniline [41].

3. Characterization of PPy-PAn/Fe_3O_4 Nanocomposite

The structure of the PPy-PAn/Fe_3O_4 nanocomposite was characterized by Fourier transform infrared (FT-IR) spectroscopy. The scanning electron microscopy (SEM) analysis was used in characterization of the morphology, determining the particle size and also distribution of the particles. Moreover, energy dispersive x-ray analysis (EDX) was performed in characterization of synthesized PPy-PAn/Fe_3O_4 nanocomposite and also comparison and approval of lead and other ions adsorbed to the nanocomposite before and after of the adsorption experiment.

4. Assay of Pb(II) Concentration

Due to investigation of samples, 10 ml Pb(II) 10 ppm solution was prepared; pH of this solution was about 5-6. To optimize the conditions of the experiment, by the use NaOH 0.1 M pH of the solution was raised to 8-10, and using water and ice bath temperature of the solution was fixed at 10 °C. After adjustment of the conditions, 20 mg of synthesize polymeric adsorbent (PPy-PAn/Fe_3O_4 nanocomposite) was added to solution and the solution was stirred for 15 mins. At the end of experiment by the use of magnet, nanocomposite was separated from solution and solution was analyzed for Pb(II) concentration.

5. Preparation of Real Sample

Real sample was prepared from the one of the zinc and lead ingot producers companies in Zinc Producers Special Zone at Zanjan County, Zanjan, Iran. Wastewater from one of the above-mentioned companies was investigated in the present study. 20 mg of synthesized nanocomposite was added to 10 ml of wastewater, which was adjusted for pH control (pH=8) and temperature of 10 °C. After 15 min nanocomposite was collected by the use of a magnet. Remaining solution was ready for determination experiments.

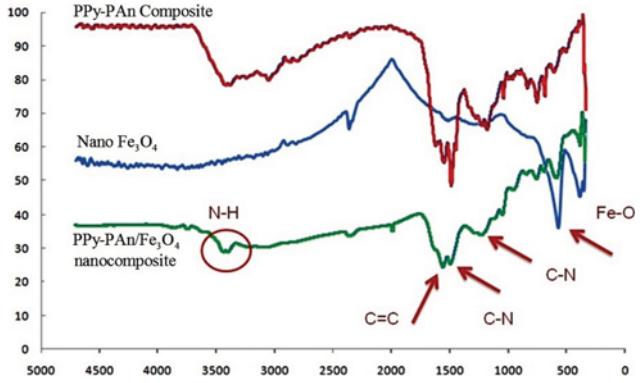

Fig. 2. FTIR spectrum of the PPy-PAn nanocomposite.

RESULTS AND DISCUSSION

1. Characterization of the PPy-PAn/Fe_3O_4 Nanocomposite

To confirm the synthesis of PPy-PAn/Fe_3O_4 nanocomposite, FTIR analysis was done and is shown in Fig. 2. The FTIR spectrum of the PPy-PAn nanocomposite (Fig. 2) demonstrated peaks at 3,419, 1,554, 1,627, 1,454, 1,278, 1,186 and 757 cm^{-1} that are considered to arise from polyaniline and polypyrrole N-H stretching, Polypyrrole ring C-N stretching, C=C polyaniline ring stretching, polypyrrole stretching C-H vibration, polyaniline stretching C-N vibration, respectively, C-H inner plan bending vibration for polyaniline and C-H outer plan bending vibration for polyaniline [42-45]. Fig. 1(b) shows the FTIR spectrum of Fe_3O_4 nanoparticles. As can be seen, peak at 574 confirmed the presence of Fe-O vibration, which corresponds to Fe_3O_4 nanoparticles. Fig. 1(c) demonstrates the FTIR spectrum of PPy-PAn/Fe_3O_4 nanocomposite. As can be clearly seen, this spectrum is combined of two previously discussed spectra. Peak at 582, which is related to the vibration of

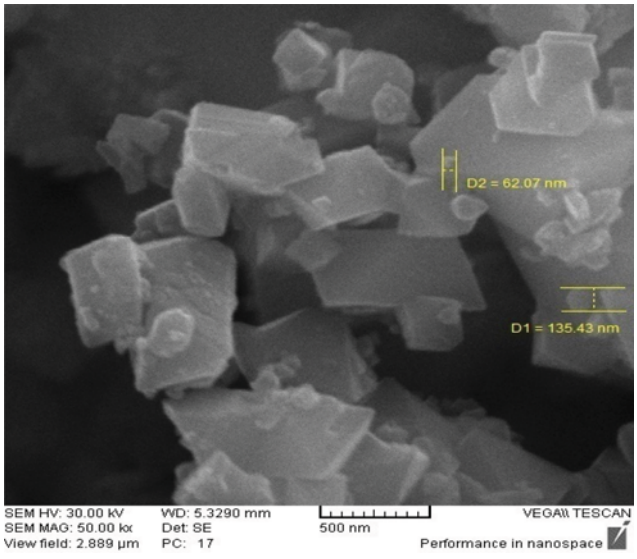

Fig. 3. SEM image of Fe_3O_4 nanoparticles (500 nm).

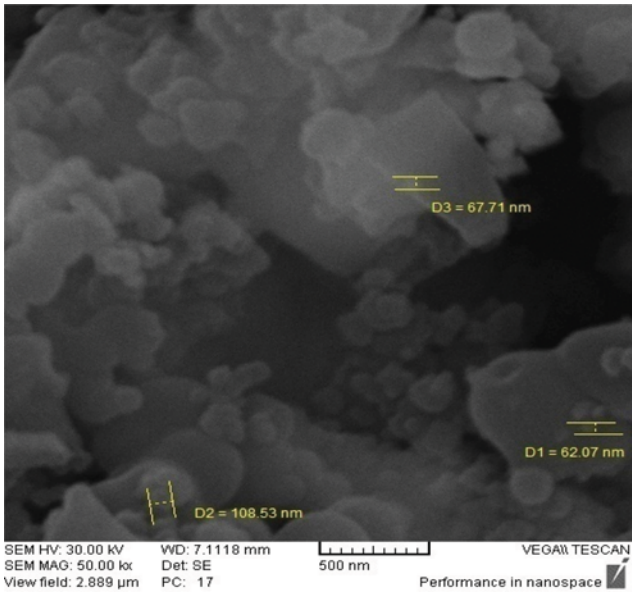

Fig. 4. SEM image of PPy-Pan/Fe_3O_4 nanoparticles (500 nm).

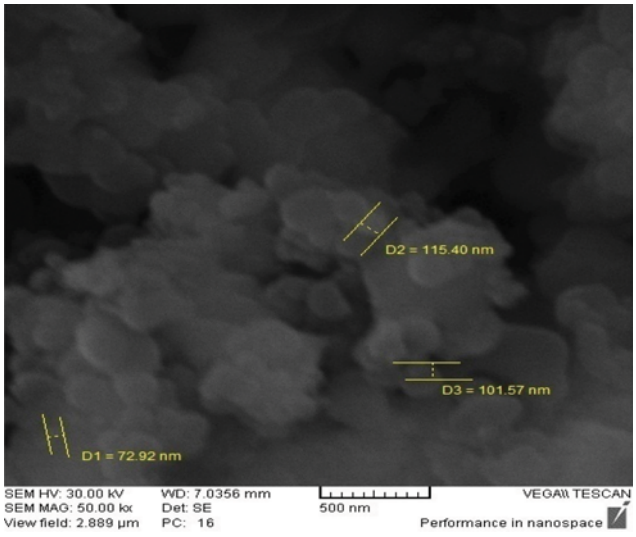

Fig. 5. SEM image of PPy-Pan/Fe_3O_4 nanoparticles after Pb(II) ions adsorption (500 nm).

Fe-O, is also demonstrated in the figure. Moreover, other related peaks are given in Fig. 2. SEM images of Fe_3O_4 nanoparticles, PPy-PAn/Fe_3O_4 nanocomposite and also PPy-PAn/Fe_3O_4 nanocomposite after Pb(II) adsorption are given in Fig. 3 to Fig. 5. SEM micrographs clearly show the synthesis of PPy-PAn/Fe_3O_4 nanocomposite. Fig. 4 shows the combination of the Fe_3O_4 nanoparticles by PPy-PAn. Fig. 4 shows the SEM image of the above-mentioned nanocomposite after absorption of the Pb ions. The figure clearly shows that by absorption of the lead ions the vast majority of the porous sites have been occupied by lead ions. Consequently, the trend of SEM images approves the absorption of Pb ions onto the PPy-PAn/Fe_3O_4 nanocomposite. In addition, 60-110 nm of diameter for the particles of the synthesized nanocomposite were detected from the analyses, which indicates better performance during the decontamination process. Energy dispersive X-ray analysis was used for nanocomposite synthesis confirmation and also characterization of elements in PPy-PAn/Fe_3O_4 nanocomposite after Pb(II) removal. EDX diagrams are illustrated in Fig. 6 and Fig. 7. Figures clearly show the removal of lead ions from solution using PPy-PAn/Fe_3O_4 nanocomposite. Outcomes demonstrate that Pb(II) ion intensity has been increased from 2 to 14. This results clearly stands on the Pb(II) removal using PPy-PAn/Fe_3O_4 nanocomposite.

2. Effect of Operational Parameters

2-1. Effect of pH

The effect of initial solution pH on Pb(II) percentage removal by

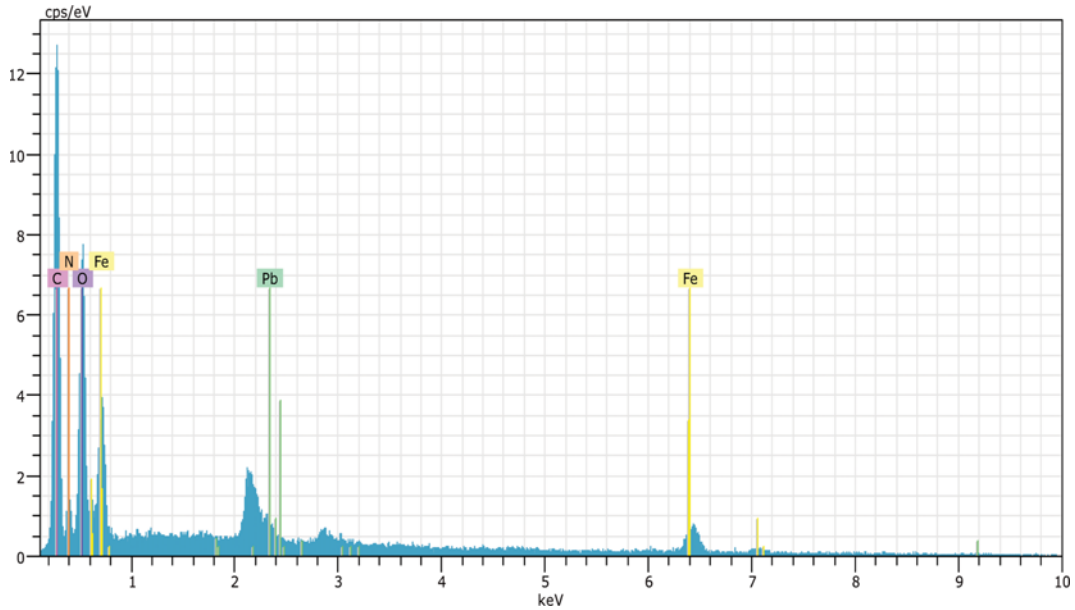

Fig. 6. EDX spectra analysis for PPy-Pan/Fe_3O_4 nanoparticles (500 nm).

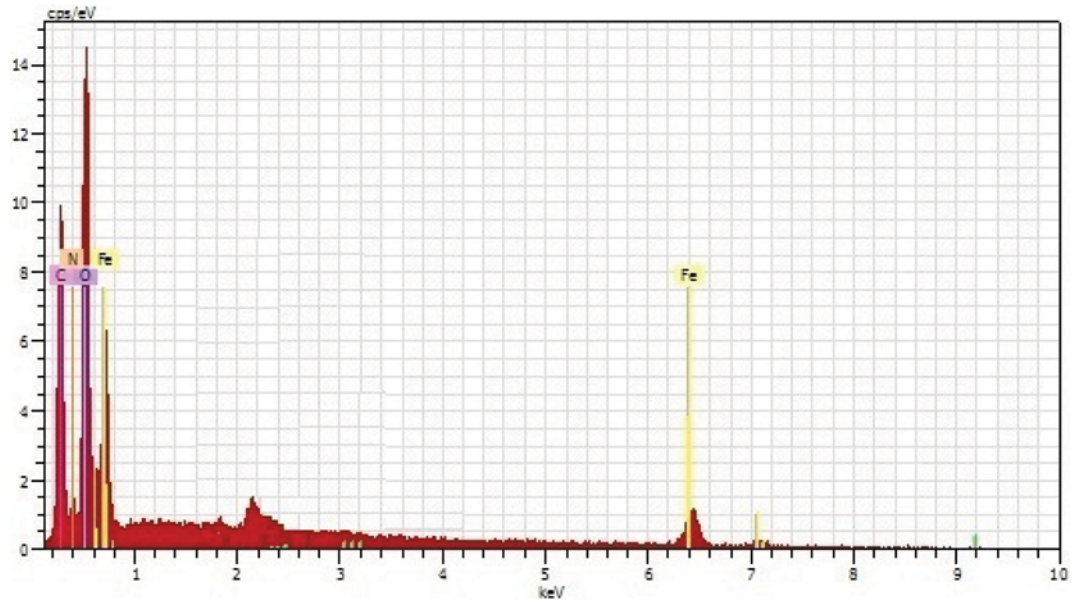

Fig. 7. EDX spectra analysis for PPy-Pan/Fe_3O_4 nanoparticles after adsorption process (500 nm).

the PPy-PAn/Fe_3O_4 nanocomposite is shown in Fig. 8. It is evident that the highest (100%) Pb(II) removal efficiency was found for the PPy-PAn/Fe_3O_4 nanocomposite. As it can be seen, by decreasing the pH, surface charge is neutralized. Consequently, reduction of Pb(II) removal efficiency under the acidic pH is due to the competitive interaction between the hydroxyl (OH^-) ions and $Pb(OH)_2$ ions for the same sorption sites on the adsorbent surface.

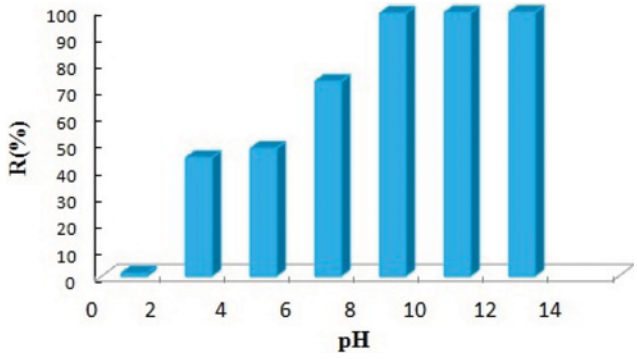

Fig. 8. Effect of pH on adsorption process, adsorbent weight: 0.02 g, solution concentration: 50 ppm, contact time: 15 mins, T= 10 °C.

2-2. Effect of Solution Initial Concentration

To study the influence of initial concentration of Pb(II), different concentrations of lead ions from 10 ppm to 300 ppm in presence of the 20 ppm of PPy-PAn/Fe_3O_4 nanocomposite were investigated. It is obviously shown in Fig. 9 that by increasing concentration of Pb(II) ions in determined amount of adsorbent, the solution removal efficiency is decreased accordingly. Most important reason for this event can explained by this point, which in low concentration of metallic ions, there are adequate spaces on the surface of adsorbent for adsorbing the ions. But, by increasing the concentration of lead Pb(II), the accessibility to the free sites on the surface of adsorbent is decreased and consequently the adsorption percentage is decreased.

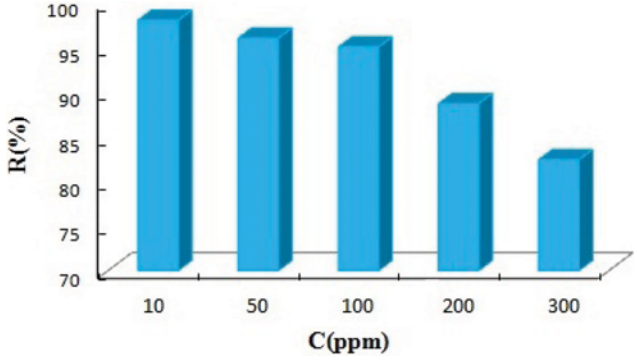

Fig. 9. Effect of solution initial concentration on adsorption process, adsorbent weight: 0.02 g, pH=8-10, contact time: 15 mins, T=10 °C.

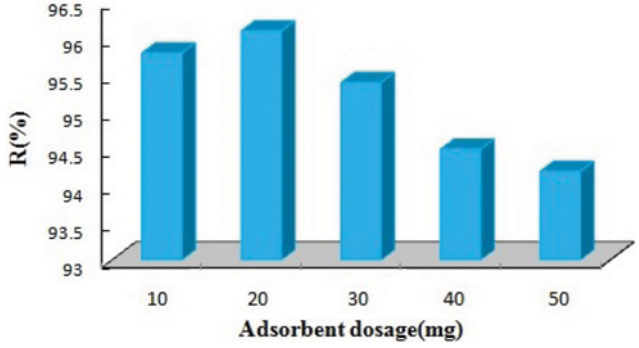

Fig. 10. Effect of adsorbent dose on adsorption process, solution concentration: 50 ppm, pH=8-10, contact time: 15 mins, T=10 °C.

2-3. Effect of Adsorbent Dose

The effect of the PPy-PAn/Fe_3O_4 nanocomposite dose on Pb(II) removal from aqueous solution is shown in Fig. 10. Experiment is done using 50 ppm solution for Pb(II) aqueous solution and 10 mg to 50 mg varying amount of adsorbent (pH=8-10). Concentration of lead ions was considered after 15 mins shaking. It is shown in Fig. 10 that Pb(II) percentage removal decreases with an increase in PPy-PAn/Fe_3O_4 nanocomposite dose. The increase in the amount of the PPy-PAn/Fe_3O_4 nanocomposite significantly influenced the lower adsorption of Pb(II) ions due to the decrease in the number of active sites available for adsorption.

2-4. Effect of Contact Time

Naturally, increasing the time of interaction leads to the increase in the amount of adsorption and removal efficiency will increased. However, the impact of reverse reactions, which lead to decreasing in the removal efficiency, after a while is more than first collisions effect. In this experiment 20 ppm dose of adsorbent and 50 ppm of pb(II) solution was used at the 60 min of the time range and time factor effect was measured at 10 min periods. Results have been illustrated in Fig. 11. As it is clear from figure, by increasing the contact time from 0 to 20 mins, adsorption efficiency is increasing. However, after the 20 mins of contact time, adsorption performance has decreased. The most important reason for this outcome

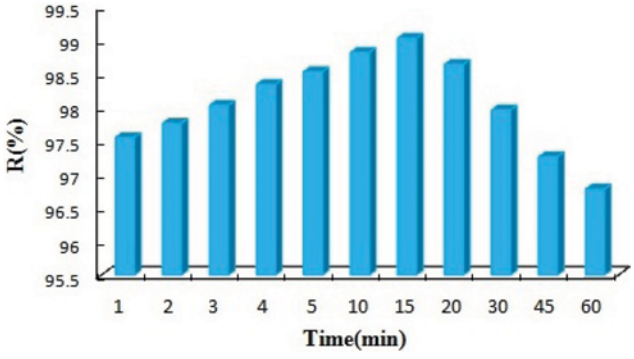

Fig. 11. Effect of contact time on adsorption process, solution concentration: 50 ppm, pH=8-10 ppm, T=10 °C.

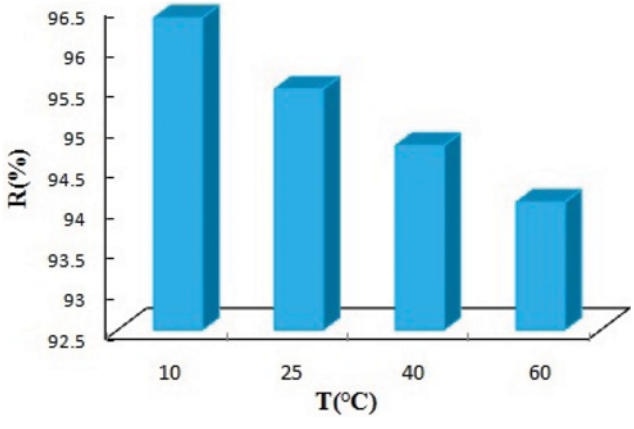

Fig. 12. Effect of temperature on adsorption process, solution concentration: 50 ppm, pH=8-10 ppm, contact time: 15 mins, T=10 °C.

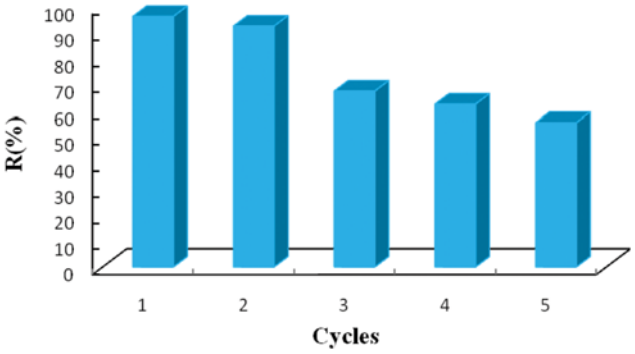

Fig. 13. Effect of repetitive usage of PPy-PAn/Fe_3O_4 nanocomposite on reusability of adsorbent.

is the effective adsorption of Pb ions at first contact; after a while all sites of the adsorbent are closed. Actually, after perfect adsorption of the Lead ions, because of the desorption procedure, reverse action (desorption) is started.

2-5. Effect of Temperature

To consider the influence of temperature parameter on the removal of Pb(II) ions from solution, the same experiment with 10 ml of 50 ppm Pb(II) ions in presence of 20 mg adsorbent in different temperatures as, 10 °C, 25 °C, 40 °C and 60 °C was repeated (pH= 8-10). Outcomes are presented in Fig. 12. As can be seen from Fig. 12, by increasing the temperature, removal percentage decreases. The main reason for this observation is that by increasing the temperature, active sites on adsorbent are weakened and physical interactions will overwhelm on the adsorption, and consequently, a decrease in adsorption and also removal efficiency is observed by temperature increasing.

3. Reusability of PPy-PAn/Fe_3O_4 Nanocomposite

To assess the reusability of the synthesized PPy-PAn/Fe_3O_4 nanocomposite, an experiment was considered based on constant amount of adsorbent. Experiments were considered based on the uses of adsorbent in five cycles. Conditions were conducted in 10 ml of 50 ppm solution of Pb(II), 10 °C temperature, 20 ppm of adsorbent dosage and 15 mins of shaking time. Results are given in Fig. 13. By using in every cycle, the removal efficiency is lowered, but the most important plus of the synthesized PPy-PAn/Fe_3O_4 nanocomposite was the reusability of this adsorbent, while after five cycles adsorption efficiency was more than 50%.

4. Real Sample Analysis

Based on the above mentioned experiments, an experiment including a real sample containing lead ions was considered. Optimum conditions of the experiments were considered for this analysis. Sample was prepared from the one of the zinc and lead producers of the province of Zanjan, Zanjan, Iran. For analysis of the sample, 10 ml of sample was selected and after pH adjustment (pH=8) and temperature (T=10 °C), 20 ppm of adsorbent was added to the solution. After 15 mins shaking, by the use of a magnet nanocomposite, was separated from the solution and Pb(II) solution was considered for analysis. An important point worthy of mentioning, the sample had polluted to other elements which contained elements of Hg^{2+} (6.12 ppm), Fe^{2+} (20.17 ppm), Zn^{2+} (2.23 ppm), Pb^{2+} (14.08 ppm). However, analysis outcomes showed that Pb(II)

removal efficiency of 88.84% resulted, which is a significant amount in presence of other species.

5. Desorption Experiment

To test the regenerability and reusability of the nanocomposite adsorbent, desorption experiments were conducted in a batch mode. For desorption of Pb(II) ions, three different media were considered. Taking into consideration the necessity of acidic media for desorption of metal ions, a desorption experiment was performed by distilled water, hydrochloric acid (HCl 0.5 M) and also nitric acid (HNO_3 0.5 M) at different concentrations. So, after preparing the mentioned solutions by defined concentrations, desorption experiments were conducted in distilled water, hydrochloric acid (0.5 M) and also nitric acid (0.5 M). Results showed that distilled water had NOT the ability of desorption of metal ions; using HCl 0.5 M, 74.41% amount of desorption and HNO_3 0.5 M, 76.32% of desorption was concluded for Pb(II) ions. Desorption experiment by HNO_3 which had the best efficiency among other media was conducted in three steps, in order to reach the most amount of desorption for Pb(II) ions. Desorption amounts for Pb(II) in three steps were 76.32%, 87.11% and 93%, respectively. Ability of the acidic media for desorption of metal ions is based on the competition of metal ions with hydrogen ions.

6. Kinetic Study

Kinetic study for the adsorption experiment using PPy-PAn/Fe_3O_4 nanocomposite was conducted in order to investigate the kinetic behavior of the adsorption process. There are many equations to study of kinetic behavior of adsorption procedures, for which pseudo-first order and pseudo-second order equations are most applicable [43]. Eq. (1) and Eq. (2) show pseudo-first order and pseudo-second order equations, respectively:

$$\log(q-q_e)=\log q_e-\frac{k_{1ads}}{2.303}t \quad (1)$$

$$\frac{t}{q}=\frac{1}{k_{2ads}q_e^2}+\frac{1}{q_e}t \quad (2)$$

where q_e and q are the amount of metal ions adsorption on adsorbent in equilibrium and in any studied times of experiments in mgL^{-1},

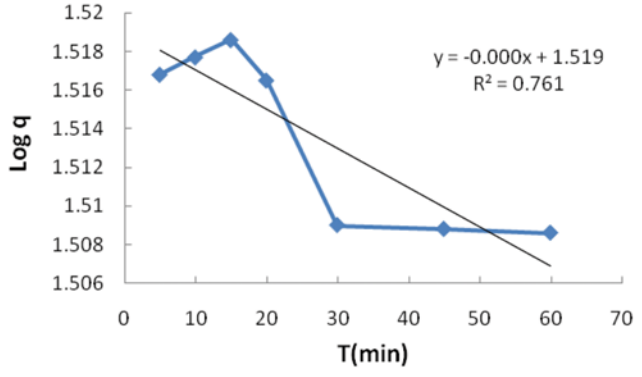

Fig. 14. Kinetic modeling of the adsorption process for lead ions by synthesized PPy-PAn/Fe_3O_4 nanocomposite using pseudo-first order kinetic equation. Operational parameters: solution concentration=50 ppm, pH=8-10 ppm, time of contact: 15 mins, T=10 °C.

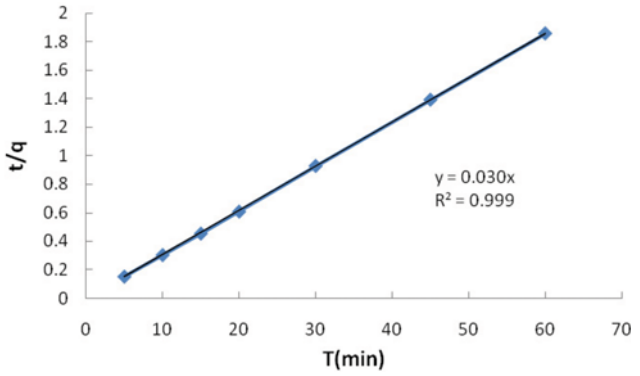

Fig. 15. Kinetic modeling of the adsorption process for lead ions by synthesized PPy-PAn/Fe_3O_4 nanocomposite using pseudo-second order kinetic equation. Operational parameters: solution concentration=50 ppm, pH=8-10 ppm, time of contact: 15 mins, T=10 °C.

respectively; k_1 is the pseudo-first order and k_2 pseudo-second order equations constants. Fig. 14 and Fig. 15 show the results of the present work approximation. As can be seen, R^2 of the equations for studying kinetics demonstrated that the pseudo-second order model is fitted better than other equations comparison by experimental outcomes.

6-1. Sorption Isotherm

To describe the interaction between an adsorbate and an adsorbent and to design and operate an adsorption system successfully, equilibrium adsorption isotherm data is important. The adsorption isotherms of Pb(II) removal by PPy-PAn/Fe_3O_4 nanocomposite at temperatures of 25 °C, 35 °C and 45 °C are shown in Fig. 5(c). It is observed that there is an increase in the uptake of Pb(II) with an increase in temperature. This may be due to an increase in thermal energy of the adsorbing species, which leads to higher adsorption capacity. This indicates that Pb(II) adsorption by the PPy-PAn/Fe_3O_4 nanocomposite is endothermic. Three extensively used isotherm models, Langmuir, Freundlich and Temkin, were employed to investigate the isotherm data. The linearized Langmuir isotherm model is represented by Eq. (3):

$$\frac{C_e}{q_e}=\frac{1}{q_{max}b}+\frac{C_e}{q_{max}} \quad (3)$$

where qm (mg/g) is the maximum adsorption capacity and b (L/mg) is the Langmuir constant related to the energy of adsorption. Furthermore, the dimensionless separation factor, R_L, which is an essential characteristic of the Langmuir model for defining the favorability of an adsorption process, was used. The R_L is given by Eq. (5);

$$R_L=\frac{1}{1+bC_0} \quad (4)$$

Based on the above equation, the linear type of Freundlich model is:

$$\log q_e=\log K_f+\frac{1}{n}\log C_e \quad (5)$$

where K_f and 1/n constants are related to the adsorption capacity

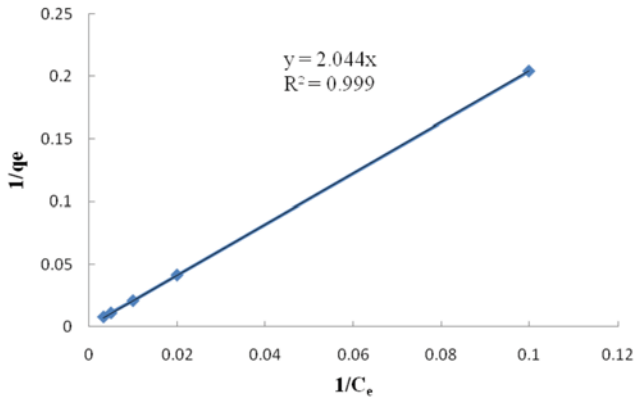

Fig. 16. Langmuir isotherm for lead ion adsorption using synthesized PPy-PAn/Fe_3O_4 nanocomposite, operational parameters: solution concentration=50 ppm, pH=8-10 ppm, time of contact: 15 mins, T=10 °C.

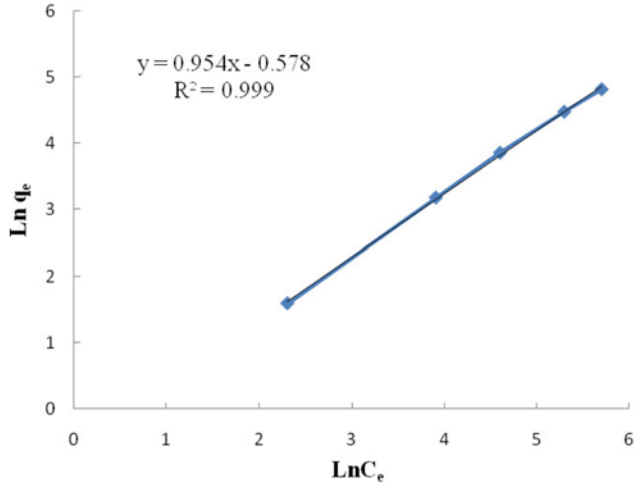

Fig. 17. Freundlich isotherm for lead ion adsorption using synthesized PPy-PAn/Fe_3O_4 nanocomposite, operational parameters: solution concentration=50 ppm, pH=8-10 ppm, time of contact: 15 mins, T=10 °C.

and intensity of adsorption, respectively. In addition, Temkin isotherm model was utilized for present work. Temkin model is considered as:

$$q_e = \frac{RT}{b}\ln(aC_e) \quad (6)$$

where A and B=RT/b are the Temkin isotherm constants, for which B is related to sorption heat index (Kjmol^{-1}). In the present work, the Temkin isotherm was investigated to describe the adsorption of Pb(II) ions onto synthesized nanocomposite. Fig. 16 to Fig. 18

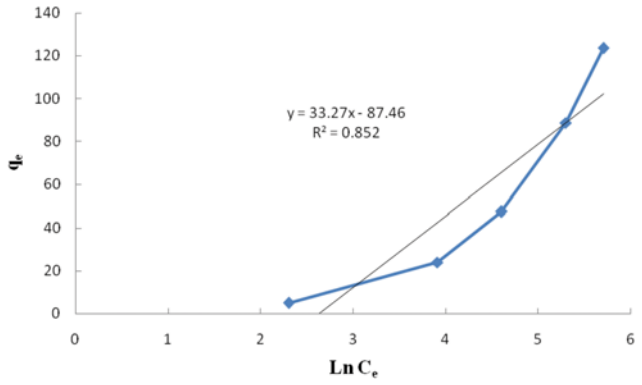

Fig. 18. Temkin isotherm for lead ion adsorption using synthesized PPy-PAn/Fe_3O_4 nanocomposite, operational parameters: solution concentration=50 ppm, pH=8-10 ppm, time of contact: 15 mins, T=10 °C.

represent the linearized Langmuir, Freundlich and Temkin isotherm plots. The Langmuir, Freundlich and Temkin isotherm parameters, which are calculated from the slope and intercept of the linear equations, are given in Table 1. The higher values of correlation coefficient reveal that Langmuir and Freundlich models fitted well the isotherm data compared to the Temkin model. The maximum adsorption capacity increases from 169.5 to 243.9 mg/g as the temperature is increased from 25 °C to 45 °C. The values of RL at different temperatures are found to be in the range 0-1, indicating that the adsorption process is favorable. Moreover, the equilibrium time for the removal of Pb(II) by the PPy-PAn/Fe_3O_4 nanocomposite is quite competitive. These results suggest that the PPy-PAn/Fe_3O_4 nanocomposite can be considered as a promising adsorbent for the removal of Pb(II) from industrial wastewater. However, more detailed adsorption mechanism approaches have been suggested and presented in some investigations [45,46].

CONCLUSION

PPy-PAn/Fe_3O_4 nanocomposite was synthesized, characterized and used as an effective adsorbent for the removal of Pb(II) form aqueous solution. The fundamental novelty of the present investigation was the utilization of polypyrrole and polyaniline together, which represented a proper performance for lead ions removal from aqueous solution. The results indicate that removal efficiency is high pH dependent and 100% removal was obtained at pH=8-10 when the initial Pb(II) concentration was 20 mg/L. Langmuir, Freundlich and Temkin isotherm models were found to describe the equilibrium isotherm data. Among these models, Freundlich isotherm model was best fitted with experimental analysis. Moreover, kinetic data fitted the pseudo-second order model. Upon using HCl

Table 1. Characteristics of the isotherms for Lead ions adsorption using synthesized PPy-PAn/Fe_3O_4 nanocomposite

Isotherm	R^2	R_L	B (L/mg)	n	K_f (mg/g)	B (KJ/mol)	a (L/g)
Langmuir	0.99	1	0.36	-	-	-	-
Freundlich	0.99	-	-	1.048	1.056	-	-
Temkin	0.852	-	-	-	-	0.074	0.069

and HNO_3, 75% PPy-PAn/Fe_3O_4 nanocomposite was achievable and could be reused for two consecutive adsorption-desorption cycles without appreciable loss of its original capacity. This work involved the use of real wastewater sample containing a number of contaminants that may affect the performance of the material. However, 84% removal of the Pb(II) ions was attained for the real sample.

REFERENCES

1. M. K. Aroua, F. M. Zuki and N. M. Sulaiman, *J. Hazard. Mater.*, **147**, 752 (2007).
2. T. N. De castro Dentas, A. A. Dantas Neto, A. De, M. C. P. Moura, E. L. Barros Neto and E. de paiva Telemaco, *Langmuir*, **17**, 4256 (2001).
3. S. A. Katz and H. Salem, *J. Appl. Toxicol.*, **13**, 217 (1993).
4. A. M. Yusof and N. A. N. N. Malek, *J. Hazard. Mater.*, **162**, 1019 (2009).
5. EPA (Environmental Protection Agency), Environmental Pollution Control Alternatives, EPA/625/5-90/025, EPA/625/4-89/023, Cincinnati (1990).
6. J. W. Patterson, *Industrial Wastewater Treatment Technology*, 2nd Ed., Butterworth-Heinemann, London (1985).
7. J. Hu, G. H. Chen and I. M. C. Lo, *Water Res.*, **39**, 4528 (2005).
8. N. R. Bishnoi, M. Bajaj, N. Sharma and A. Gupta, *Bioresour. Technol.*, **91**, 305 (2004).
9. M. Dakiky, M. Khamis, A. Manassra and M. Mereb, *Adv. Environ. Res.*, **6**, 533 (2002).
10. T. Vidhyadevi, M. Arukkani, K. Selvaraj, P. Manickam Periyaraman, R. Lingam and S. Subramanian, *Korean J. Chem. Eng.*, **32**, 650 (2015).
11. A. Rahmani, D. Nematollahi, G. Azarian, K. Godini and Z. Berizi, *Korean J. Chem. Eng.*, **32**(8), 1570 (2015).
12. K. Selvi, S. Pattabhi and K. Kadirvelu, *Bioresour. Technol.*, **80**, 87 (2001).
13. D. Mohan, K. P. Sing and V. K. Sing, *Ind. Eng. Chem. Res.*, **44**, 1027 (2005).
14. B. Sandhya and A. K. Tonni, *Chemosphere*, **54**, 951 (2004).
15. W. Daoud, T. Ebadi and A. Fahimifar, *Korean J. Chem. Eng.*, **32**, 1119 (2015).
16. H. Li, Z. Li, T. Liu, X. Xiao, Z. Peng and L. Deng, *Bioresour. Technol.*, **99**, 6271 (2008).
17. R. Chand, K. Narimura, H. Kawakita, K. Ohto, T. Watari and K. Inoue, *J. Hazard. Mater.*, **163**, 245 (2009).
18. E. Alvarez-Ayuso, A. Garcia-Sanchez and X. Querol, *J. Hazard. Mater.*, **142**, 191 (2007).
19. V. Goshu, Y. V. Tsarev and V. V. Kastrov, *Russ. J. Appl. Chem.*, **82**, 801 (2009).
20. S. Debnath and U. C. Ghosh, *J. Chem. Thermodyn.*, **40**, 67 (2008).
21. S. Goswami and U. C. Ghosh, *Water SA*, **31**, 597 (2005).
22. L. A. Rodrigues, L. J. Maschio, R. E. da Silva and M. L. C. Pinto da Silva, *J. Hazard. Mater.*, **173**, 630 (2010).
23. D. R. Mulinari, G. L. J. P. Siva and M. L. C. P. Silva, *Quim. Nova*, **29**, 496 (2006).
24. N. Savage and M. S. Diallo, *J. Nanopart. Res.*, **7**, 331 (2005).
25. X. Zhao, Y. Shi, Y. Cai and S. Mou, *Environ. Sci. Technol.*, **42**, 1201 (2008).
26. A. F. Ngomsik, A. Bee, M. draye, G. Cote and V. Cabuil, *Comptes Rendus Chimie*, **8**, 963 (2005).
27. L. Li, M. Fan, R. C. Brown, L. J. HansVan, J. Wang, W. Wang, Y. Song and P. Zhang, *Crit. Rev. Environ. Sci. Technol.*, **36**, 405 (2006).
28. R. C. O'Handley, *Modern Magnetic Materials: Principles and Applications*, John Wiley and Sons, New York (2000).
29. J. Hu, I. M. C. Lo and G. Chen, *Water Sci. Technol.*, **50**, 139 (2004).
30. Y. Peng, D. Liu, M. Fan, D. Yang, R. Zhu, F. Ge, J. Zhu and H. He, *J. Hazard. Mater.*, **173**, 614 (2010).
31. J. Hu, I. M. C. Lo and G. Chen, *Langmuir*, **21**, 11173 (2005).
32. T. M. Wu and S. H. Lin, *J. Polym. Sci. Part B: Polym. Phys.*, **44**, 1413 (2006).
33. G. Han, J. Yuan, G. Shi and F. Wei, *Thin Solid Films*, **474**, 64 (2005).
34. X. Zhang and R. Bai, *Langmuir*, **19**, 10703 (2003).
35. X. Zhang, R. Bai and Y. W. Tong, *Sep. Purif. Technol.*, **52**, 161 (2006).
36. B. Saoudi, N. Jammul, M. L. Abel, M. M. Chehimi and G. Dodin, *Synth. Met.*, **87**, 97 (1997).
37. A. Mollahosseini, *Electrochemical Coating and Characterization of Polyphosphate-doped Polypyrrole on Steel Surface, and its Applications in SPE and SPME*, A Dissertation Submitted as a Partial Fulfillment of the Requirements for the Degree of Doctor of Philosophy in Analytical Chemistry, April (2009).
38. A. Samzadeh-Kermani and S. Miri, *Korean J. Chem. Eng.*, **32**, 1137 (2015).
39. G. S. Akundy, R. Rajagopalan and J. O. Iroh, *J. Appl. Poly. Sci.*, **83**, 1970 (2002).
40. C. H. Cho, H. J. Choi, J. W. Kim and M. S. Jhon, *J. Mater. Sci.*, **39**, 1883 (2004).
41. M. Bhaumik, T. Y. Leswifi, A. Maity, V. V. Srinivasu and M. S. Onyango, *J. Hazard. Mater.*, **186**, 150 (2011).
42. M. Bhaumik, A. Maity, V. V. Srinivasu and M. S. Onyango, *J. Hazard. Mater.*, **190**, 381 (2011).
43. Y. Yu, C. Ouyang, Y. Gao, Z. Si, W. Chen, Z. Wang and G. Xue, *J. Polym. Sci. Part A: Polym. Chem.*, **43**, 6105 (2005).
44. A. Maity and S. Sinha Ray, *Macro-mol. Rapid Commun.*, **29**, 1582 (2008).
45. M. Bhaumik, H. J. Choi, R. I. McCrindle and A. Maity, *J. Colloid Interface Sci.*, **425**, 75 (2014).
46. N. Ballav, H. J. Choi, S. B. Mishra and A. Maity, *J. Ind. Eng. Chem.*, **20**, 4085 (2014).